

Counterfactual Explanation via Search in Gaussian Mixture Distributed Latent Space

Xuan Zhao¹, Klaus Broelemann¹, Gjergji Kasneci²

¹SCHUFA Holding AG

²Technical University of Munich

xuan.zhao@schufa.de, klaus.broelemann@schufa.de, gjergji.kasneci@tum.de

Abstract

Counterfactual Explanations (CEs) are an important tool in Algorithmic Recourse for addressing two questions: 1. What are the crucial factors that led to an automated prediction/decision? 2. How can these factors be changed to achieve a more favorable outcome from a user’s perspective? Thus, guiding the user’s interaction with AI systems by proposing easy-to-understand explanations and easy-to-attain feasible changes is essential for the trustworthy adoption and long-term acceptance of AI systems. In the literature, various methods have been proposed to generate CEs, and different quality measures have been suggested to evaluate these methods. However, the generation of CEs is usually computationally expensive, and the resulting suggestions are unrealistic and thus non-actionable. In this paper, we introduce a new method to generate CEs for a pre-trained binary classifier by first shaping the latent space of an autoencoder to be a mixture of Gaussian distributions. CEs are then generated in latent space by linear interpolation between the query sample and the centroid of the target class. We show that our method maintains the characteristics of the input sample during the counterfactual search. In various experiments, we show that the proposed method is competitive based on different quality measures on image and tabular datasets – efficiently returns results that are closer to the original data manifold compared to three state-of-the-art methods, which are essential for realistic high-dimensional machine learning applications.

1 Introduction

In contemporary society, the widespread adoption of machine learning models is evident, with a growing emphasis on the need for transparency, particularly in critical domains such as healthcare, finance, and employment. The ability to comprehend the behavior of these models is essential for instilling trust in decision-making systems rooted in machine learning. Various methodologies have been devised by researchers to

elucidate the connections between a model’s input and output. While simpler models like logistic regression, decision trees, and rule fit algorithms allow for direct interpretation, more intricate models necessitate analysis through the lens of simpler surrogate models. An additional avenue of investigation focuses on addressing a fundamental query within a binary classification context: “How can one modify the input to generate a prediction favoring the preferred class over the unfavored one?” This exploration, known as counterfactual analysis, involves examining outcomes in alternative yet similar non-occurring scenarios [Menzies and Beebe, 2020]. When working with a pre-trained and fixed model, the sole method for altering the model’s output is by modifying the input. Counterfactual explanations (CEs) serve as prescriptive recommendations regarding the features of the queried sample (i.e., input) that need adjustment (along with the magnitude of the required changes) to attain the desired result. It is essential for these changes to be minimal (associated with low costs) and feasible (realistic). With clear semantic implications and a common logical foundation, CEs are generally comprehensible for end-users [Fernandez *et al.*, 2020]. In fact, in the literature, the most direct application of CEs often involves providing guidance to end-users.

However, CEs have their downsides. High-dimensional input spaces lead to high-dimensional CEs with limited utility for the potential users of the explanation (less intuitive and less feasible). In addition, searching through the high-dimensional space for CEs is computationally expensive. Other than the problem caused by the dimensionality, without proper constraints, it is possible to generate out-of-sample CEs close to the original data distribution. Out-of-sample CEs can result in explanations/suggestions that are not feasible (i.e., unlikely to be achieved since they do not correspond to the training data distribution). Adversarial samples [Goodfellow *et al.*, 2015] which resemble the original sample but have changed imperceptibly to fool the classifier, might be a good example to illustrate this situation even though they are designed for a different purpose (deceive human perception and pre-trained classifiers). We show in Section 4 that a search in the original space for CEs might cause this situation. An feasible CE should stay close to the data manifold and suggest meaningful (i.e., realistic and easily achievable) changes to a query sample. Various requirements are proposed in the literature for generating useful CEs: feasi-

ble, sparse, valid, proximate, and computationally efficient to generate [Verma *et al.*, 2020]. It is also clear that there might be a trade-off between these requirements.

We introduce a method for generating CEs by using interpolation within the latent representations of the input data to achieve the requirements mentioned above. We perform experiments with an image dataset – MNIST and two tabular datasets – the Adult income and Lending Club loan default. Our main contributions are: (1) a model agnostic framework for finding feasible CEs that are prominent in scalability in data with a low computational expense, (2) a novel strategy for manipulating the latent space for the counterfactual search, (3) a comparison of methods across the image and tabular datasets.

The remainder of this paper is structured as follows: First, we briefly review the existing methods of counterfactual explanation (Section 2). Then, in Section 3, we propose a CE method via autoencoder-aided search in Gaussian Mixture (GM) distributed latent space. In Section 4, we present the evaluation results of our method against three state-of-the-art methods. Finally, Section 5 concludes the paper.

2 Background and Related Work

2.1 Generating Counterfactuals by Perturbing the Original Input Space

A substantial portion of the existing literature focuses on generating counterfactuals by perturbing the input feature space. In the realm of inverse classification [Lash *et al.*, 2017], sparsity is preserved by categorizing features into immutable and mutable ones, subjecting the latter to budgetary constraints. An alternative approach, proposed by [Laugel *et al.*, 2017], employs the growing spheres method for sampling to traverse the input space and identify Counterfactual Explanations (CEs). Utilizing gradient descent in the input space, [Dhurandhar *et al.*, 2018] seeks contrastive explanations, categorizing them into pertinent positives and pertinent negatives, and incorporating an autoencoder loss to ensure explanations remain within the sample.

Further enhancements to gradient descent methods involve the introduction of prototypes, guiding the descent towards the average value of the target class by averaging representations in the latent space from the training sets [Van Looveren and Klaise, 2020]. GRACE [Le *et al.*, 2020] is specifically tailored for neural networks on tabular data, combining contrastive explanations with interventions through constrained gradient descent. It adds an extra loss, measuring information gain, to maintain sparse resulting explanations. Many of the aforementioned methods already incorporate generative models to stay within the sample. The Explainable Artificial Intelligence (XAI) criteria for CEs are integrated into these methods, either as constraints or as the backbone of the loss design, which may pose challenges for optimization, particularly in high-dimensional input scenarios.

2.2 Generating Counterfactuals by Perturbing the Latent Space

Methods that perturb input features lacking proper regularization may yield unconvincing and impractical counterfactuals,

bearing a resemblance to adversarial samples [Goyal *et al.*, 2019]. To tackle this issue, employing latent space perturbation methods proves promising, as they integrate generative and probabilistic models into the algorithm design, ensuring that counterfactuals align with a high probability under the data distribution $p(X)$. An illustrative instance is StyleEx [Lang *et al.*, 2021], wherein the classifier is incorporated into the generative model, manipulating the latent space to facilitate the visualization of counterfactual searches.

ExplainGAN [Samangouei *et al.*, 2018] offers another approach, focusing on generating counterfactual explanations for images. This method involves training multiple autoencoders and leveraging signals from classifiers and discriminators to inform the learned representations. Counterfactuals are then generated through a growing sphere search in the latent space of a conditional variational autoencoder [Pawelczyk *et al.*, 2020]. In a different vein, [Guyomard *et al.*, 2021] creates counterfactuals using class prototypes derived from a supervised auto-encoder, a unique aspect being the use of supervised auto-encoders for obtaining these prototypes.

For gradient descent in the latent space of a variational autoencoder, regularization terms are applied to enhance the process [Balasubramanian *et al.*, 2021]. Despite their efficacy, these methods may incur computational expenses. An alternative, Sharpshooter [Barr *et al.*, 2021], employs linear interpolation in the latent space with the assistance of two distinct autoencoders, presenting a less costly approach. However, it does not guarantee the preservation of label-irrelevant features in the counterfactual search.

3 Our method

3.1 Problem Setting

Our method requires access to the dataset and a previously trained classifier that we want to explain with counterfactual explanations. We only consider a binary classification in this paper. In the problem setting of counterfactual explanation, there is usually a base class where instances belong that class wants to seek feasible counterfactual explanation toward the target class. The dataset is composed $\mathcal{D} = (x_i, y_i)_{i=1}^K$ where we can split x into two classes where x_i belongs to the base class has $\hat{y}_i = 0$ and x_i belongs to the target class has $\hat{y}_i = 1$ under the classifier $\hat{y} = f(x)$. x_q is a query sample with an output 0 from the classifier f . 1 is the desired target output. Hence, CEs are needed for the query sample x_q under the classifier f .

3.2 Desiderata for CE Search

Our approach is driven by the following main desiderata:

Desideratum 1 The exploration process must preserve intrinsic and label-irrelevant attributes of the input query. This implies that the attainment of the target label should rely on the inherent properties of the input and demand minimal effort.

Desideratum 2 The generation step should produce counterfactual explanations (CEs) that are notably realistic, ensuring feasibility.

Desideratum 3 Efficient retrieval of CEs is essential, especially in high-dimensional scenarios, to guarantee practical

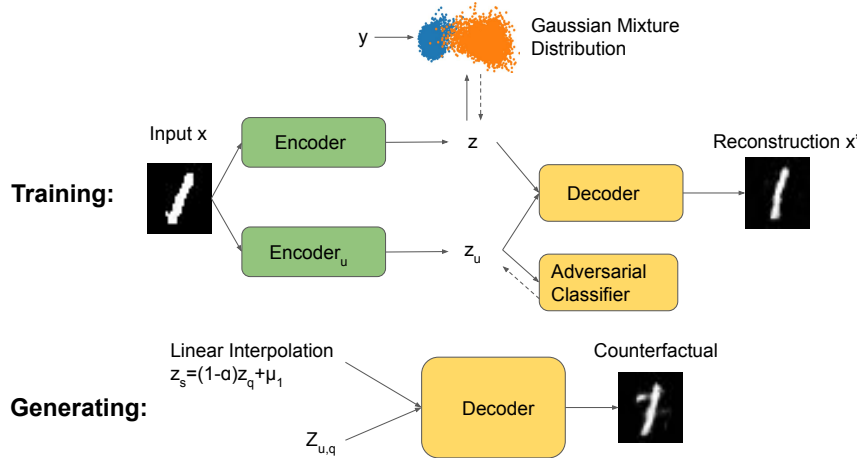


Figure 1: Diagram of the data flow in the algorithm. During Training: an input sample x from the training dataset is embedded in a latent space with a Gaussian mixture distribution by the Encoder. x is also embedded into a latent space to get z_u learned by the Encoder_u with an Adversarial Classifier that helps remove the information related to the classification label \hat{y} of x under the pre-trained classifier f . z and z_u are then combined to get reconstruction x' . During Generating: x_q is a certain query sample we need to explain with CE. z_q is Encoder(x_q) and μ_1 is the mean of target class in latent space z . A linear search is performed in the latent space of z to get a searched potential z_s (a is a parameter that controls the interpolation). Then z_s and $z_{u,q}$ are projected back to the original space by the Decoder until the decision boundary of the classifier is crossed.

applicability in real-life situations.

3.3 Learning Components

We design a CE generation method based on two main steps: a Training Step in which we use the same training dataset used in training the classifier to learn an autoencoder with its latent space shaped by enforcing a Gaussian-mixture distribution on the embeddings and a Generating Step in which we use interpolation in the latent space to find a relatively less computational expensive counterfactual explanation. The algorithm flow is shown in Figure 1. It only requires access to the training dataset and prediction of the pre-trained classifier f that we aim to explain through appropriate CEs. For our Training Step, we form a new training dataset $\mathcal{D}_t = (x_i, \hat{y}_i)_{i=1}^K$ by replacing original y in \mathcal{D} with \hat{y} .

In the following part of this subsection, we will describe each component of the Training Step in Figure 1. The details of Generating Step are described in Section 3.4.

Label Relevant Branch: Gaussian Mixture Distribution

Gaussian Mixture models are usually used in a unsupervised way, but in our usage, it is supervised by the classification label produced by the pre-trained classifier. Our goal for generating a CE is to cross the decision boundary of the pre-trained classifier by taking advantage of Gaussian mixture distribution in the latent space, in which case, we could generate a CE without having a process of optimization for each query sample. Intuitively, in the latent space, data points with the same class label should cluster closer to each other. Inspired by GM loss [Wan *et al.*, 2018], we could use a classification constraint and likelihood constraints to 'push' the latent space to a Gaussian mixture distribution for further manipu-

lation. After proper training, we could 'force' the extracted embedding z on the training set following a Gaussian mixture distribution expressed in Equation 1, in which μ_c and σ_c are the mean and covariance of class c in the latent space, and $p(c)$ is the prior probability of class c . In the binary classification setting, $c \in [0, 1]$.

$$p(z) = \sum_c p(z | c)p(c) = \sum_c \mathcal{N}(z; \mu_c, \sigma_c)p(c) \quad (1)$$

If the latent space follows a Gaussian mixture distribution, the conditional probability distribution of a latent embedding z given its class label c can be expressed in Equation 2. The corresponding posterior probability distribution can be expressed in Equation 3.

$$p(z | c) = \mathcal{N}(z; \mu_c, \sigma_c)p(c) \quad (2)$$

$$p(c | z) = \frac{\mathcal{N}(z; \mu_c, \Sigma_c)p(\mu_c)}{\sum_{c=1}^C \mathcal{N}(z; \mu_c, \sigma_c)} \quad (3)$$

A **classification loss** \mathcal{L}_{cls} is then calculated as the cross-entropy between the posterior probability distribution and the class label as is shown in Equation 4.

$$\mathcal{L}_{cls} = -\frac{1}{N} \sum_{i=1}^N \log \frac{\mathcal{N}(z_i; \mu_{\hat{y}}, \Sigma_{\hat{y}})p(\mu_{c=\hat{y}})}{\sum_{c=1}^C \mathcal{N}(z_i; \mu_c, \Sigma_c)} \quad (4)$$

Applying the classification loss only cannot reach our goal of forcing the latent space to be a Gaussian mixture distribution. There will be situations where a z_i can be far away from the corresponding target class centroid μ_c and still be correctly classified since it is relatively closer to μ_c than to the

means of the other classes in multiple classifications—which could be an outlier. To fix this problem, we then use a likelihood to measure the extent to of the training data fits the Gaussian mixture distribution. The **likelihood** for $\{z, c\}$ is expressed in Equation 5. The likelihood could serve as a constraint to the original classification loss.

$$\mathcal{L}_{lkd} = - \sum_{i=1}^N \log \mathcal{N}(z_i; \mu_{z_i}, \Sigma_{z_i}) \quad (5)$$

Gaussian mixture loss \mathcal{L}_{GM} we optimize to update the parameters of Encoder, μ_c and Σ_c , during Step 1, is defined in Equation 6, in which λ is a weighting coefficient.

$$\mathcal{L}_{GM} = \mathcal{L}_{cls} + \lambda_{lkd} \mathcal{L}_{lkd} \quad (6)$$

Label Irrelevant Branch: Encoder_u and Adversarial Classifier We notice that generative models usually try to generate various unseen samples. However, the generation of CEs needs to satisfy different criteria, as mentioned in Section 1. In our problem setting, to satisfy *Desideratum 1*, which requires maintaining the characteristics of the query sample during the search, it is intuitive to adopt disentanglement methods in the latent space of an autoencoder.

Inspired by a Two-Step Disentanglement Method [Hadad *et al.*, 2020], we introduce an Adversarial Classifier to ensure that the embedding z_u captured by the Encoder_u is classification label-irrelevant. It is inspired by GANs, where the discriminator gradually loses the capacity to tell the generated data from the real data during the training phase. While GANs are usually used to improve the quality of generated output – telling fake from real, the adversarial component in our design encourages the Encoder_u to dismiss information about the labels, leading to disentanglement. With the Adversarial Classifier, we could guarantee that the z_u and \hat{y} are disentangled and independent, which prepares for the interpolation in the Generating Step. \hat{y}' is the classification label of z_u through the Adversarial Classifier. The **adversarial classification loss** is shown in Equation 7 as binary cross entropy loss.

$$\mathcal{L}_{adv} = -\frac{1}{N} \sum_{i=1}^N \hat{y}_i \log \hat{y}'_i + (1 - \hat{y}_i) \log(1 - \hat{y}'_i) \quad (7)$$

Autoencoder The reconstruction error of the autoencoder is shown in Equation 8.

$$\mathcal{L}_{rec} = \frac{1}{N} \sum_{i=1}^N \|x_i - x'_i\|^2 \quad (8)$$

Summary The configuration of the network in the Training Step is composed of three network branches: first, in the **Label Relevant Branch**, the \mathcal{L}_{GM} forces z to be Gaussian Mixture Distribution. Second, in the **Label Irrelevant Branch**, the Adversarial Classifier is trained to minimize the **adversarial classification loss** \mathcal{L}_{adv} in Equation 7 – it is trained to classify z_u to \hat{y} . Third, the autoencoder network is trained to minimize the **total loss** \mathcal{L} , the sum of three terms as shown in Equation 9: (i) the **reconstruction loss** \mathcal{L}_{rec} as shown in

Algorithm 1 Training Step of our proposed architecture

Require: ψ, π, ϕ and ω the initial parameters of Encoder, Encoder_u, Decoder and Adversarial Classifier; μ_c and Σ_c the initial mean and covariance of the Gaussian distribution of z ; n the number of iterations; λ_{lkd} and λ_{adv} the weights of regularization terms \mathcal{L}_{lkd} and \mathcal{L}_{adv} ; $c \in [0, 1]$

- 1: **while** not converged **do**
- 2: **for** $i = 0$ to n **do**
- 3: Sample $\{x, y\}$ a batch from dataset \mathcal{D}_t .
- 4: $\omega \stackrel{\pm}{\leftarrow} -\nabla_{\omega} \mathcal{L}_{adv}$
- 5: $\mathcal{L}_{GM} \leftarrow \mathcal{L}_{cls} + \lambda_{lkd} \mathcal{L}_{lkd}$
- 6: $\psi, \mu_c, \Sigma_c \stackrel{\pm}{\leftarrow} -\nabla_{\psi, \mu_c, \Sigma_c} (\mathcal{L}_{GM} - \lambda_{adv} \mathcal{L}_{adv})$
- 7: Sample $\{x, y\}$ a batch from dataset \mathcal{D}_t .
- 8: $\mathcal{L} \leftarrow \mathcal{L}_{rec} + \lambda_{lkd} \mathcal{L}_{lkd} - \lambda_{adv} \mathcal{L}_{adv}$
- 9: $\psi, \pi, \phi \stackrel{\pm}{\leftarrow} -\nabla_{\psi, \pi, \phi} \mathcal{L}$
- 10: **end for**
- 11: **end while**

Algorithm 2 Generating Step of our proposed architecture

Require: S samples $\alpha = \alpha_{s=1}^S$ in $(0, 1]$; x_q the query sample; x_s potential CE; f classifier; tol tolerance; T probability of target counterfactual class (0.5 for decision boundary); μ_1 the mean of target class in latent space of the label relevant branch

- 1: $z_q \leftarrow Encoder(x_q)$
- 2: $z_{u,q} \leftarrow Encoder_u(x_q)$
- 3: **for** α_s in α **do**
- 4: $z_s = (1 - \alpha)z_q + \alpha\mu_1$
- 5: $x_s \leftarrow Decoder(z_s, z_{u,q})$
- 6: **if** $|f(x_s) - T| < tol$ **then**
- 7: $x_{cf} = x_s$
- 8: **end if**
- 9: **end for**
- 10: **return** x_{cf}

Equation 8, (ii) **likelihood** in Equation 5 and (iii) minus the **adversarial classification loss** \mathcal{L}_{adv} in Equation 7.

$$\mathcal{L} = \mathcal{L}_{rec} + \lambda_{lkd} \mathcal{L}_{lkd} - \lambda_{adv} \mathcal{L}_{adv} \quad (9)$$

3.4 Algorithm

Algorithm 1 and 2 show pseudo code to process our method in addition to Figure 1 which is used to generate the counterfactual in Section 4.

For the Training Step, we sample a batch from the training dataset to update the parameters of Adversarial Classifier ω , Encoder ψ and mean and covariance μ_b, μ_t , and σ_b, σ_t – base class and target class combined as training data. Then we sample another batch to update the Encoder, Encoder_u, and Decoder parameters together (ψ, π , and ϕ). We iterate this procedure until convergence of the loss functions is reached. During the end of the Training Step: we should get a **label relevant** latent space z following Gaussian Mixture distribution (see Figure 4 for PCA of z in Appendix) and a **label irrelevant** latent space z_u to capture the label irrelevant information of samples. In Generating Step, where we



Figure 2: Original and counterfactual samples for MNIST showing from top to bottom: original query images and CEs found via Our Method, GDL, Prototype and RL. Note Our Method exhibits more combination of the characteristics of the original query samples (e.g., tilt and thickness of the strokes) and the target label than the other methods. Our Method and GDL remain (perturbation in latent space) more realistic than the Prototype and RL (perturbation in original space).

generate a CE of a query sample x_q . We first pass x_q from the base class through the Encoder and the Encoder $_u$ to obtain the sample’s embeddings z_q and $z_{u,q}$. Then we get the searched potential z_s by linear interpolation in latent space: $z_s = (1 - \alpha)z_q + \alpha\mu_1$ (α in $(0, 1]$), where μ_1 is the mean of target class in latent space of the label relevant branch. z_s and $z_{u,q}$ combined are decoded through the Decoder to get x_s , and the pre-trained classifier f assesses its classification score. The counterfactual search stops if it crosses the decision boundary and is within a user (end-user or developer of the algorithm) specified tolerance tol , which is the desired maximum distance from T for the generated counterfactual’s classification score. For the experiments in Section 4, the decision boundary T is set to be 0.5. The search is performed by sampling along the line with a finite number of α .

Note that we demonstrate our method in the scenario with binary decision. However, it is straight-forward to extend our method to handle a multi-categorical decision.

4 Experiments and Evaluation

We compare our method to three other counterfactual methods introduced in Section 2: Gradient Descent Method improved with Prototypes (Prototype) [Van Looveren and Klaise, 2020], CE Generation with Reinforcement Learning (RL) [Samoilescu *et al.*, 2021] and Gradient Descent in the Latent Space of a VAE (GDL) [Balasubramanian *et al.*, 2021] on three datasets: MNIST [LeCun *et al.*, 1998] (image), Adult Dataset [Kohavi and Becker, 1996] (tabular) and Lending Club [Yash, 2020] (tabular). The reason why we choose Prototype and RL is that they are both designed not only for image datasets but also for tabular datasets. Besides, they both use autoencoders to learn the representation to remain close to the data distribution, similar to our design, while they use other constraints to ensure desiderata like sparsity. We use the package ALIBI [Klaise *et al.*, 2021] for Prototype and RL to stay close to the original design. GDL is a relatively simple baseline, but it is similar to our method because both operate in latent space. We implement GDL from

Table 1: Summary of metrics for MNIST

Method	time(s)	reconstruction	sparsity	validity(%)	proximity
Our Method	0.007±0.001	0.012±0.003	2.119 ±0.857	89.5	0.193 ±0.075
GDL	1.568 ±0.047	0.247 ±0.048	2.121 ±0.085	77.9	0.172±0.068
Prototype	1.345 ±0.095	0.926 ±0.175	0.014±0.005	58.7	1.075±0.055
RL	0.085 ±0.012	0.857±0.058	0.015±0.026	60.5	0.834±0.047

Table 2: Summary of metrics for Adult income

Method	time(s)	reconstruction	sparsity	validity(%)	proximity
Our Method	0.008±0.002	0.012±0.005	0.343±0.127	90.3	0.193±0.045
GDL	1.568±0.224	0.520±0.135	0.090±0.002	84.2	2.170±0.835
Prototype	7.345±0.784	4.463±0.563	0.014±0.005	75.3	1.075±0.235
RL	1.804±0.112	5.453±0.673	0.012±0.008	65.3	0.875±0.132

scratch since the source code is not available. Our networks are trained on an Intel(r) Core(TM) i7-8700 CPU and the networks in our experiments are built based on Pytorch [Paszke *et al.*, 2019]

4.1 Measures for Comparison

We evaluate the quality of CEs by the measures taken from literature [Verma *et al.*, 2020; Barr *et al.*, 2021; Wachter *et al.*, 2018]: (i) **counterfactual generation time**, time required to find a CE for a given query sample (ii) **validity**, the percentage success in generating CEs that the target labels requested by the users are reached (iii) **proximity**, distance(L_2 norm) from query samples to CEs in original space (iv) **sparsity**, L_1 norm of the change vector in original space (v) **reconstruction loss** – a measure of the CE being in sample. We pass a CE through the autoencoder and measure its loss. A smaller loss indicates closer to the original data distribution because the autoencoder is trained on the same training dataset as the pre-trained classifier. Further details about the metrics used in the experiments can be found in the appendix.

4.2 Datasets, Training and Evaluation

MNIST The MNIST database is a large database of hand-written digits. For MNIST, we adjust the problem as a binary classification problem of predicting ones (our base class) and sevens (our target class) while the original problem setting is multi-classification. MNIST provides a naturally intuitive visualization of the result of a gradual change from the base class to the target class crossing the decision boundary given a query sample. The counterfactual generated shown in Figure 3 exhibits a combination of characteristics from the query sample (e.g., the tilt of long-stroke) and from the target class (e.g., longer leveled stroke in sevens). Our *Desideratum 1* – generating a CE while keeping the characteristics of the query sample which are not related to the classification prediction is reached. In our problem setting with MNIST, the tilt and length of long strokes of query sample ones are kept during the interpolation process. Table 1 (mean±SD) shows the quality of counterfactual explanations as measured by the above metrics. Our method outperforms the other methods in time, reconstruction, and validity but not in proximity and sparsity (very close to GDL in proximity, though). Our method

outperforms Prototype and RL in the time dimension since it searches through the latent space with lower dimensions. It is also more substantial than GDL because it performs interpolation instead of optimization for a single query sample. It indicates that our method is suitable for high-dimensional applications which require intensive computation.

For MNIST, we use a CNN-based network, and we train the model for 20 epochs by stochastic gradient descent using the Adam optimizer and a batch size of 100 on the training dataset. Our model uses two hyperparameters, λ_{adv} and λ_{lkd} , for regularizing the loss functions for the network. We varied λ_{adv} and λ_{lkd} between 0.01 and 1 during training. During the training process, we want the three loss terms \mathcal{L}_{adv} , \mathcal{L}_{lkd} and \mathcal{L}_{cls} to remain approximately on the same scale. We found $\lambda_{adv} = 0.05$ and $\lambda_{lkd} = 0.1$ to give us a numerical balance among the three loss terms by checking the testing dataset. We use these values to report our results. The details of the hyper-parameters of the Discriminator are shown in the Appendix.

ADULT The Adult dataset was drawn from the 1994 United States Census Bureau data. It used personal information such as education level and working hours per week to predict whether an individual earns more or less than \$50,000 per year [Kohavi, 1996]. We train a classifier with age, years of education, capital gain, capital loss, hours-per-week as continuous features, and education level as a categorical feature for simplicity (considering mutable and immutable features are not the focus of this paper). The dataset is imbalanced – the instances made less than \$50,000 constitute 25% of the dataset, and the instances made more than \$50,000 constitute 75% of the dataset. To avoid the situation that the accuracy of the classifier for an imbalanced dataset only reflects the distribution of the training dataset, we train a classifier with re-weighting according to the proportion of base and target class. For tabular datasets, more preprocessing is performed compared to image datasets. We normalize the continuous features and use one-hot encoding to deal with the categorical features for the input of the autoencoder. We train the model for 100 epochs by stochastic gradient descent using the Adam optimizer and a batch size of 100. λ_{adv} and λ_{lkd} are set at 0.05 and 0.5. For tabular datasets, we use a multi-layer perceptron-based network. The details of the

Table 3: Summary of metrics for Lending Club default loan

Method	time(s)	reconstruction	sparsity	validity(%)	proximity
Our Method	0.007±0.001	0.132±0.081	1.713±0.627	92.1	3.532±0.258
GDL	3.569 ±0.087	0.142 ±0.046	1.731 ±0.068	76.3	1.652±0.668
Prototype	3.137 ±0.915	0.546 ±0.235	1.016±0.035	75.7	1.975±1.045
RL	0.035 ±0.042	0.673±0.124	1.017±0.076	67.5	1.034±0.127

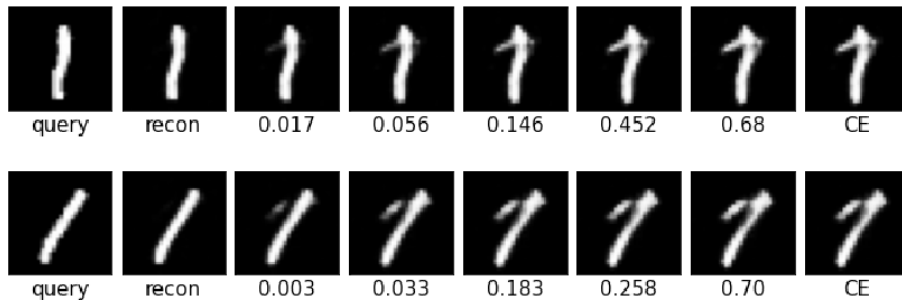


Figure 3: the gradual changes and classification scores for query samples along the interpolation path. Along the paths, the label irrelevant characteristics (e.g., tilt and thickness of the strokes) stay.

architectures of the networks for the Adult income dataset are shown in the appendix. Based on the comparison results shown in Table 2, our method outperforms in time, reconstruction dimensions and proximity, while RL is stronger in sparsity. Intuitively, perturbation in original space without much guidance could quickly end up as adversarial samples [Goodfellow *et al.*, 2015], which provide non-actionable CEs. In contrast, operations in latent space (our method and GDL) could be closer to the original datasets.

Lending Club Lending Club is a peer-to-peer lending company that allows individuals to lend to other individuals [Lending Club, 2020]. This tabular dataset includes whether a borrower defaulted on their loan size, annual income, debt-to-income ratio, FICO score, loan length, etc. We train a classifier to predict default using five continuous and one categorical feature. Since this dataset is also imbalanced – the default class constitutes around 15% of the population, we adjust the loss functions of the classifier and the autoencoder to re-weighted versions based on the proportion of each class. From Table 3, we find that similar to the Adult income dataset, our method is much faster at generating CEs and excels at reconstruction and validity. The training details of this dataset are similar to ADULT. Furthermore, more details are included in the Appendix.

5 Conclusion

This paper presents a novel model-agnostic algorithm for finding CEs via linear interpolation in latent space. Our method implements a framework that first disentangles the label relevant and label irrelevant dimensions and then searches in a Gaussian mixture distributed latent space of the label relevant latent dimensions for CEs given a query sample. We demonstrated our method’s advantages and disadvantages by comparing it to three similar methods (GDL, Prototype and RL) on three different datasets (MNIST, ADULT income, and

Lending Club default loan). We show that our method is faster and provides more valid CEs which are closer to the original dataset (in the dimensions of time, validity and reconstruction). Based on the presented comparison, we suggest that our work could evolve around improving latent representation.

Acknowledgement

This work has received funding from the European Union’s Horizon 2020 research and innovation programme under Marie Skłodowska-Curie Actions (grant agreement number 860630) for the project “NoBIAS - Artificial Intelligence without Bias”.

References

- [Balasubramanian *et al.*, 2021] Rachana Balasubramanian, Samuel Sharpe, Brian Barr, Jason Wittenbach, and C. Bayan Bruss. Latent-CF: A Simple Baseline for Reverse Counterfactual Explanations. *arXiv:2012.09301 [cs]*, June 2021.
- [Barr *et al.*, 2021] Brian Barr, Matthew R. Harrington, Samuel Sharpe, and C. Bayan Bruss. Counterfactual Explanations via Latent Space Projection and Interpolation. *arXiv:2112.00890 [cs]*, December 2021.
- [Dhurandhar *et al.*, 2018] Amit Dhurandhar, Pin-Yu Chen, Ronny Luss, Chun-Chen Tu, Paishun Ting, Karthikeyan Shanmugam, and Payel Das. Explanations based on the missing: Towards contrastive explanations with pertinent negatives. In *Proceedings of the 32nd International Conference on Neural Information Processing Systems, NIPS’18*, pages 590–601, Red Hook, NY, USA, December 2018. Curran Associates Inc.

- [Fernandez *et al.*, 2020] Carlos Fernandez, Foster Provost, and Xintian Han. Full Text: Explaining Data-Driven Decisions made by AI Systems: The Counterfactual Approach. <https://onikle.com/articles/48299>, January 2020.
- [Goodfellow *et al.*, 2015] Ian J. Goodfellow, Jonathon Shlens, and Christian Szegedy. Explaining and Harnessing Adversarial Examples. *arXiv:1412.6572 [cs, stat]*, March 2015.
- [Goyal *et al.*, 2019] Yash Goyal, Ziyang Wu, Jan Ernst, Dhruv Batra, Devi Parikh, and Stefan Lee. Counterfactual Visual Explanations. *arXiv:1904.07451 [cs, stat]*, June 2019.
- [Guyomard *et al.*, 2021] Victor Guyomard, Françoise Fessant, Tassadit Bouadi, and Thomas Guyet. Post-hoc counterfactual generation with supervised autoencoder. In Michael Kamp, Irena Koprinska, Adrien Bibal, Tassadit Bouadi, Benoît Frénay, Luis Galárraga, José Oramas, Linara Adilova, Yamuna Krishnamurthy, Bo Kang, Christine Langeron, Jeffrey Lijffijt, Tiphaine Viard, Pascal Welke, Massimiliano Ruocco, Erlend Aune, Claudio Gallicchio, Gregor Schiele, Franz Pernkopf, Michaela Blott, Holger Fröning, Günther Schindler, Riccardo Guidotti, Anna Monreale, Salvatore Rinzivillo, Przemyslaw Biecek, Eirini Ntoutsi, Mykola Pechenizkiy, Bodo Rosenhahn, Christopher L. Buckley, Daniela Cialfi, Pablo Lanillos, Maxwell Ramstead, Tim Verbelen, Pedro M. Ferreira, Giuseppina Andresini, Donato Malerba, Ibéria Medeiros, Philippe Fournier-Viger, M. Saqib Nawaz, Sebastián Ventura, Meng Sun, Min Zhou, Valerio Bitetta, Ilaria Bordino, Andrea Ferretti, Francesco Gullo, Giovanni Ponti, Lorenzo Severini, Rita P. Ribeiro, João Gama, Ricard Gavaldà, Lee A. D. Cooper, Naghmeh Ghazaleh, Jonas Richiardi, Damian Roqueiro, Diego Saldana Miranda, Konstantinos Sechidis, and Guilherme Graça, editors, *Machine Learning and Principles and Practice of Knowledge Discovery in Databases - International Workshops of ECML PKDD 2021, Virtual Event, September 13-17, 2021, Proceedings, Part I*, volume 1524 of *Communications in Computer and Information Science*, pages 105–114. Springer, 2021.
- [Hadad *et al.*, 2020] Naama Hadad, Lior Wolf, and Moni Shahar. A Two-Step Disentanglement Method. *arXiv:1709.00199 [cs, stat]*, January 2020.
- [Klaise *et al.*, 2021] Janis Klaise, Arnaud Van Looveren, Giovanni Vacanti, and Alexandru Coca. Alibi Explain: Algorithms for Explaining Machine Learning Models, June 2021.
- [Kohavi and Becker, 1996] Ronny Kohavi and Barry Becker. UCI Machine Learning Repository: Adult Data Set. <https://archive.ics.uci.edu/ml/datasets/adult>, 1996.
- [Kohavi, 1996] Ron Kohavi. Scaling up the accuracy of Naive-Bayes classifiers: A decision-tree hybrid. In *Proceedings of the Second International Conference on Knowledge Discovery and Data Mining, KDD'96*, pages 202–207, Portland, Oregon, August 1996. AAAI Press.
- [Lang *et al.*, 2021] Oran Lang, Yossi Gandelsman, Michal Yarom, Yoav Itzhak Wald, Gal Elidan, Avinatan Hassidim, Bill Freeman, Phillip Isola, Amir Globerson, Michal Irani, and Inbar Mosseri. Explaining in Style: Training a GAN to explain a classifier in StyleSpace. In *Proc. ICCV 2021*, 2021.
- [Lash *et al.*, 2017] Michael T. Lash, Qihang Lin, W. Nick Street, and Jennifer G. Robinson. A budget-constrained inverse classification framework for smooth classifiers. *arXiv:1605.09068 [cs, stat]*, June 2017.
- [Laugel *et al.*, 2017] Thibault Laugel, Marie-Jeanne Lesot, Christophe Marsala, Xavier Renard, and Marcin Detryniecki. Inverse Classification for Comparison-based Interpretability in Machine Learning. *arXiv:1712.08443 [cs, stat]*, December 2017.
- [Le *et al.*, 2020] Thai Le, Suhang Wang, and Dongwon Lee. GRACE: Generating Concise and Informative Contrastive Sample to Explain Neural Network Model's Prediction. *arXiv:1911.02042 [cs, stat]*, October 2020.
- [LeCun *et al.*, 1998] Yann LeCun, Corinna Cortes, and Christopher Burges, J.C. Handwritten Digit Database. <http://yann.lecun.com/exdb/mnist/>, 1998.
- [Lending Club, 2020] Lending Club 2007-2020Q3. <https://www.kaggle.com/datasets/ethon0426/lending-club-20072020q1>, 2020.
- [Menzies and Beebe, 2020] Peter Menzies and Helen Beebe. Counterfactual Theories of Causation. In Edward N. Zalta, editor, *The Stanford Encyclopedia of Philosophy*. Metaphysics Research Lab, Stanford University, winter 2020 edition, 2020.
- [Paszke *et al.*, 2019] Adam Paszke, Sam Gross, Francisco Massa, Adam Lerer, James Bradbury, Gregory Chanan, Trevor Killeen, Zeming Lin, Natalia Gimelshein, Luca Antiga, Alban Desmaison, Andreas Kopf, Edward Yang, Zachary DeVito, Martin Raison, Alykhan Tejani, Sasank Chilamkurthy, Benoit Steiner, Lu Fang, Junjie Bai, and Soumith Chintala. Pytorch: An imperative style, high-performance deep learning library. In *Advances in Neural Information Processing Systems 32*, pages 8024–8035. Curran Associates, Inc., 2019.
- [Pawelczyk *et al.*, 2020] Martin Pawelczyk, Johannes Haug, Klaus Broelemann, and Gjergji Kasneci. Learning Model-Agnostic Counterfactual Explanations for Tabular Data. *Proceedings of The Web Conference 2020*, pages 3126–3132, April 2020.
- [Samangouei *et al.*, 2018] Pouya Samangouei, Ardavan Saeedi, Liam Nakagawa, and Nathan Silberman. ExplainGAN: Model Explanation via Decision Boundary Crossing Transformations. In *ECCV (10)*, January 2018.
- [Samoilescu *et al.*, 2021] Robert-Florian Samoilescu, Arnaud Van Looveren, and Janis Klaise. Model-agnostic and Scalable Counterfactual Explanations via Reinforcement Learning, June 2021.
- [Van Looveren and Klaise, 2020] Arnaud Van Looveren and Janis Klaise. Interpretable Counterfactual Explanations Guided by Prototypes. *arXiv:1907.02584 [cs, stat]*, February 2020.

[Verma *et al.*, 2020] Sahil Verma, John Dickerson, and Keegan Hines. Counterfactual Explanations for Machine Learning: A Review. *arXiv:2010.10596 [cs, stat]*, October 2020.

[Wachter *et al.*, 2018] Sandra Wachter, Brent Mittelstadt, and Chris Russell. Counterfactual Explanations without Opening the Black Box: Automated Decisions and the GDPR, March 2018.

[Wan *et al.*, 2018] Weitao Wan, Yuanyi Zhong, Tianpeng Li, and Jiansheng Chen. Rethinking Feature Distribution for Loss Functions in Image Classification. *arXiv:1803.02988 [cs]*, March 2018.

[Yash, 2020] Yash. Lending Club 2007-2020Q3. <https://www.kaggle.com/datasets/ethon0426/lending-club-20072020q1>, 2020.

.1 Metrics for Comparison

We evaluate the quality of counterfactuals by the metrics taken from literature: 1) time - time required to find a counterfactual for a query sample. Time is one of the most significant strengths of our method. We use the time spent to generate a counterfactual explanation for a query sample on average. Our approach is particularly fast compared to other methods because generating a CE requires a search through a relatively lower dimension and projection through the decoder for no more than a fixed number of interpolated points (search stops when criteria are met). By comparison, iterative search based on gradients or perturbing in the input space can be quite expensive if the search distance is large, the learning rate is low, or the mutable dimensions are high. We do not include the time of training the autoencoder with Gaussian mixture latent space due to the fact that this training time is not trivial. It is a one-time cost and is not related to the scalability of CEs generation for a query sample. Ideally, our method triumphs even more, when the query sample is high dimensional. 2) validity - the percentage of success in generating counterfactuals cross the decision boundary. The goal for generating counterfactuals is that they are counterfactuals, which requires them to be classified as the target class. We evaluate validity by including the pre-trained classifier in the algorithm. Since linear search is performed with the classifier is ended when certain criteria are met for the classifier. We could see, in general, that the performance of this dimension for the three methods is satisfying since all three methods employ the classifier as the end search criteria. 3) proximity - a measure of distance from query sample to counterfactual in latent space. Proximity is used as a constraint to promote the performance of counterfactual generation [Verma *et al.*, 2020]. This metric measures how close a counterfactual is to the query sample it is generated from. Usually, this measure is calculated by the $L2$ norm in the input space. 4) sparsity - a measure of features changed. Sparsity is a common metric in the counterfactual literature [Verma *et al.*, 2020]. Sparsity is a measure of how sparse the change vector is. We calculate the $L1$ norm of the change vector in input space. 5) reconstruction loss - a measure of the CE being close to data manifold [Barr *et al.*, 2021]. We can measure the closeness of a CE to its original dataset by passing a counterfactual through the

autoencoder and measuring its reconstruction loss. During the training process of the autoencoder, we try to minimize the reconstruction loss. Intuitively, a sample with a smaller loss should be more in-sample and closer to the original data distribution. An unseen sample should have a larger reconstruction loss concerning the autoencoder.

.2 PCA of latent space

.3 Further Thoughts about the Comparison Results

We could see that our method performs better on three dimensions above: counterfactual generation time, validity and reconstruction loss due to its design. We design the architecture based on our three desiderata and in the end, through the experiment, we show that the desiderata are achieved. Our method performs linear interpolation in the latent space instead of optimization in the original space, it has the highest validity, and also because the linear interpolation happens in latent space, we cannot guarantee the sparsity and proximity in the original space as shown in the tables, which is stated in Section 2.

.4 Algorithms of GDL

In GDL, instead of updating parameters of DNN which is commonly applied, we update the input query sample and the latent projection of the query sample correspondingly until it cross the decision boundary and the tolerance is satisfied.

Algorithm 3 Gradient Descent Latent Space

Require: ψ and ϕ the initial parameters of Encoder and Decoder; f classifier; x_b the query sample; tol tolerance; p probability of target counterfactual class (0.5 for decision boundary)

```

1:  $z_b \leftarrow \psi(x)$ 
2:  $z_t \leftarrow z_b$ 
3:  $z_t \leftarrow \nabla_{z_t}^+ (T - f(\phi(z)))^2$ 
4:  $x_t \leftarrow \phi(z_t)$ 
5: if  $|f(x_t) - T| < tol$  and  $f(x_t) > p$  then
6:    $x_{cf} = \phi(z_t)$ 
7:   return  $x_{cf}$ 
8: end if

```

.5 Repetition

We repeat experiments on each dataset five times. Before each repetition, we randomly split data into training data (80%) and test data (20%) for the computation of the standard errors of the metrics.

.6 Details of Autoencoders and Classifier

We tabulate the detailed structures of autoencoders and classifiers during experiment in Section 4. For tabular datasets, to avoid break the differentiation of $(T - f(\phi(z)))^2$, instead of argmax for decoder output, we apply temperature annealing softmax to have a sharper reconstructed sample where we set $t = 0.5$.

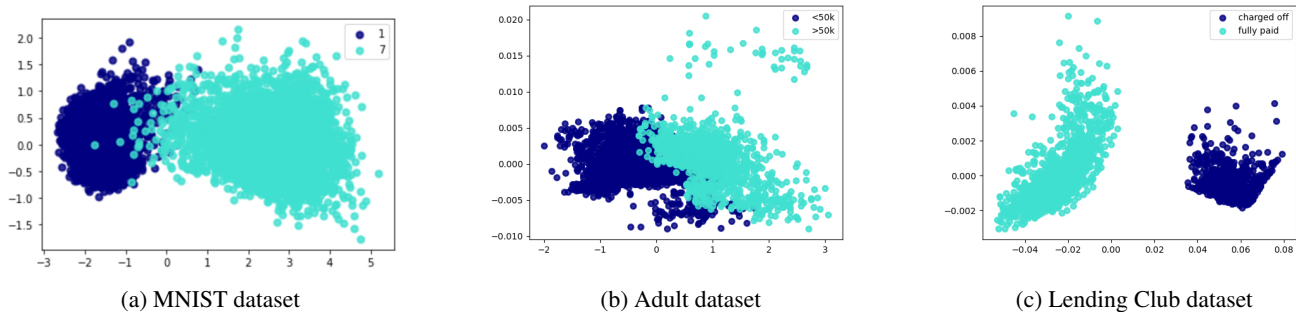


Figure 4: PCA of the base and target class in latent space

Table 4: The network structure of MNIST classifier

Input 28*28
Linear 28*28-128, ReLu
Linear 128-64, ReLu
Linear 64-32, ReLu
Linear 32-1, Sigmoid

Table 5: The network structure of Adult income autoencoder

Encoder	Decoder
Input(1,28,28)	Linear(25,128), Relu
Conv2d(1,8,2), stride 1, ReLu	Linear(128, 29*29*32), unflatten
Conv2d(8,16,2), stride 1, BatchNorm2d 16,ReLu	convtranspose2d(32,16,2),stride 1, batchnorm2d 16, ReLu
Conv2d(16,32,2), stride 1, Leaky ReLu, flatten	convtranspose2d(16,8,2),stride 1, batchnorm2d 8, ReLu
Linear(22912, 128), ReLu,	convtranspose2d(8,1,2), stride 1, sigmoid
Linear(128,15)	output(1,28,28)

The structure of Encoder_{*u*} is similar to Encoder but with the last layer of 25 nodes.

Table 6: The network structure of Adult income classifier

Input x (cont_in 6 + cat_in 16/one-hot encoding)
Linear 21-10, ReLu
Linear 10-4, ReLu
Linear 4-2, ReLu
Linear 2-1, Sigmoid

Table 7: The network structure of Adult income autoencoder

Encoder	Decoder	
Input x (cont_in 6/min-max + cat_in 16/one-hot encoding)	Linear 3-6, LeakyReLu	
Linear 21-12, LeakyReLu	Linear 6-12, LeakyReLu	
Linear 12-24, LeakyReLu	Linear 12-24, LeakyReLu	
Linear 24-12, LeakyReLu	Linear 24-5, Tanh	Linear 24-16, softmax
Linear 12-6, LeakyReLu	cont_output 5	cat_output 16
Linear 6-3		